Specific Requirements for Cytochrome *c*-550 and the Manganese-Stabilizing Protein in Photoautotrophic Strains of *Synechocystis* sp. PCC 6803 with Mutations in the Domain Gly-351 to Thr-436 of the Chlorophyll-Binding Protein CP47[†]

Tim R. Morgan, Jackie A. Shand, Shannon M. Clarke, and Julian J. Eaton-Rye*

Department of Biochemistry, University of Otago, P.O. Box 56, Dunedin, New Zealand

Received February 19, 1998; Revised Manuscript Received June 3, 1998

ABSTRACT: The requirement of cytochrome *c*-550 (PSII-V) in photosystem II (PSII) has been assessed in *Synechocystis* sp. PCC 6803 containing mutations between Gly-351 and Thr-436 of the loop E domain of the chlorophyll *a*-binding protein CP47. Six photoautotrophic strains were utilized to compare the effect of removal of either the manganese-stabilizing protein (PSII-O) or PSII-V on PSII activity in vivo. These were a wild-type control; two strains with amino acid deletions, Δ(R384-V392) and Δ(G429-T436); and three carrying specific amino acid substitutions, G351L/T365Q, G351L/E364Q/T365Q, and G351L/E353Q/E355Q/T365Q. The removal of PSII-O prevented the assembly of PSII in Δ(G429-T436) but not in Δ(R384-V392). Neither Δ(G429-T436) nor Δ(R384-V392) could support photoautotrophic growth in the absence of PSII-V. In chloride-limiting conditions, the photoautotrophic growth of Δ(R384-V392) was severely impaired and that of Δ(G429-T436) totally inhibited, and no strains lacking PSII-V could grow in chloride-limiting or calcium-limiting media. Substitutions at Gly-351, Glu-353, Glu-355, and Thr-365 produced phenotypes that were similar to those of the control in the presence or absence of PSII-O and PSII-V, but removal of PSII-O from G351L/E364Q/T365Q produced a significant reduction of assembled PSII centers and an enhanced sensitivity to photoinactivation while removal of PSII-V prevented photoautotrophic growth. The additional mutants E364Q:ΔPSII-V and E364G:ΔPSII-V demonstrated that this inhibition was a consequence of the mutation at Glu-364. These results also show that the removal of PSII-V, in vivo, produces phenotypes in the CP47 mutants examined that are either similar or more severe than those resulting from the removal of PSII-O.

The initial step in oxygenic photosynthesis is the light-driven oxidation of water by photosystem II (PSII)[1] which is present in photosynthetic eukaryotes and cyanobacteria. This multisubunit protein complex catalyzes the transfer of electrons from water to plastoquinone with the intact photosystem containing as many as 20 protein subunits in vivo with additional pigment-binding antenna proteins present that transfer absorbed excitation energy to PSII (*1*, *2*). A manganese-containing unit is ligated by the water-oxidizing complex of the photosystem and participates in the accumulation of oxidizing equivalents required for the splitting of two water molecules to yield four electrons, four protons, and molecular oxygen (*3*).

The minimum number of protein subunits required for water oxidation has not yet been established, but at least seven membrane-spanning proteins are known to be present in current PSII core preparations (*1*). These are the chlorophyll *a*-binding core antenna proteins CP47 and CP43, the reaction center D1 and D2 proteins, the α and *β* subunits of cytochrome *b*-559, and the *psb*I gene product; however, the *psb*I gene product is not essential for PSII function in the cyanobacterium *Synechocystis* sp. PCC 6803 (*4*). In addition, several nuclear-encoded hydrophilic proteins are important.

Three hydrophilic proteins located on the lumenal face of the PSII complex have been extensively characterized, and this work has been reviewed by Seidler (*5*). Of these, the PSII-O protein, encoded by *psb*O, has been shown to stabilize the manganese cluster of the water-oxidizing complex (*6*−*8*), while the two additional proteins, PSII-P and PSII-Q, encoded by *psb*P and *psb*Q, respectively, are known to participate in calcium and chloride binding (*7*, *9*, *10*). In the non-green plant PSII complexes, the PSII-P and PSII-Q proteins are absent, but two different proteins, PSII-V or cytochrome *c*-550, and PSII-U, a 12 kDa protein in *Synechocystis* sp. PCC 6803, are found (*11*, *12*).

A well-established interaction exists between the PSII-O protein and the chlorophyll *a*-binding antenna protein, CP47 (*13*). The CP47 protein is thought to possess 6 membrane-spanning helices with its N-terminus and C-terminus located on the stromal or cytosolic side of the thylakoid. There are, therefore, 3 hydrophilic loops protruding into the lumen, the largest of which, designated as loop E, comprises ap-

[†] This work has been supported by a New Zealand Marsden grant (UOO-521) to J.J.E.-R.

* To whom correspondence should be addressed.

[1] Abbreviations: bp, base pair(s); Chl, chlorophyll; HEPES, 4-(2-hydroxyethyl)-1-piperazineethanesulfonic acid; kb, kilobase(s); OD, optical density; PCC, Pasteur Culture Collection; PCR, polymerase chain reaction; PSI, photosystem I; PSII, photosystem II; SDS−PAGE, sodium dodecyl sulfate−polyacrylamide gel electrophoresis; TES, 2-[tris(hydroxymethyl)methyl]amino-1-ethanesulfonic acid; Tris, tris-(hydroxymethyl)aminomethane.

S0006-2960(98)00404-8 CCC: $15.00
Published on Web 09/23/1998

proximately 190 amino acids (*13*). In spinach, it has been shown that the C-terminal half of loop E cross-links to the N-terminal 76 amino acids of the PSII-O protein (*14*). Earlier studies had established that PSII-O protects loop E from digestion by trypsin and labeling by the amino acid modifier *N*-hydrosuccinimidobiotin while the domain Pro-361 to Ser-391 in loop E uniquely interacts with a monoclonal antibody, referred to as FAC2, when all extrinsic proteins and the manganese of the water-oxidizing complex have been removed (*15*−*17*). In the cyanobacterium *Synechocystis* sp. PCC 6803, insertional mutagenesis or deletion mutagenesis of *psb*B, the gene encoding CP47, results in the absence of PSII from the thylakoid membrane (*18*, *19*). It therefore appears that CP47 has both structural and functional roles within the water-oxidizing complex in addition to its role in energy transfer to the reaction center.

An interesting difference exists for the requirement of PSII-O between *Chlamydomonas reinhardtii*, where PSII contains PSII-P and PSII-Q, and *Synechocystis* sp. PCC 6803 or *Synechococcus* sp. PCC 7942, where PSII-V and PSII-U are present. A nuclear mutation resulting in the absence of mRNA for the PSII-O protein in *C. reinhardtii* was found to be lethal (*20*), but deletion of *psb*O in cyanobacteria did not prevent photoautotrophic growth although an enhanced sensitivity to photoinactivation was observed (*21*−*24*). In *Synechocystis* sp. PCC 6803, the deletion of *psb*V also resulted in a photoautotrophic phenotype, but the double mutant lacking both *psb*O and *psb*V was found to be an obligate photoheterotroph (*11*, *25*). These results suggest that the role of PSII-V is of a similar significance to that of PSII-O in the photosystems where it is present.

In light of these results, we have investigated the interaction of the PSII-O and PSII-V proteins with the region of loop E between Gly-351 and Thr-436. Since the extrinsic proteins have been shown to be involved with the binding of calcium and chloride, we have also investigated our mutant strains in calcium-limiting and chloride-limiting media. For these experiments, we have made use of deletions within the *psb*B gene encoding CP47. Our results reveal that different mutations within loop E respond differently when either PSII-O, the manganese-stabilizing protein, or PSII-V, the cytochrome *c*-550, is removed and have enabled us to demonstrate that Glu-364 in CP47 is required for normal PSII stability and/or assembly in the absence of either of these components of the cyanobacterial photosystem.

MATERIALS AND METHODS

Propagation of Synechocystis sp. PCC 6803. *Synechocystis* sp. PCC 6803 cultures were maintained on BG-11 plates in the presence of 5 mM glucose, 20 μM atrazine, and the appropriate antibiotics which prevented spontaneous reversion in the mutant strains (*26*, *27*). The antibiotics used were spectinomycin at 25 μg/mL, kanamycin at 25 μg/mL, and erythromycin at 25 μg/mL. The BG-11 solid medium was supplemented with 10 mM TES−NaOH, pH 8.2, and 0.3% sodium thiosulfate. The liquid cultures were grown mixotrophically in the presence of antibiotics and 5 mM glucose unless noted otherwise. All cultures were maintained at 30 °C under constant illumination of 25 $\mu E \cdot m^{-2} \cdot s^{-1}$ provided by two 250 W General Electric metal halide bulbs and were aerated with filtered air using an aquarium pump.

Growth Curves. Photoautotrophic and photoheterotrophic growth curves were started by cultures that had been grown mixotrophically to an OD at 730 nm of approximately 1.0. These cells were harvested by centrifugation at 2675*g* for 10 min and washed twice in the appropriate BG-11 growth medium supplemented with 25 mM HEPES−NaOH, pH 7.5. Photoheterotrophic growth curves were performed in the presence of 20 μM diuron and 5 mM glucose. Measurements were taken at 730 nm every 12 or 24 h, and cells were always diluted to an OD at 730 nm of less than 0.4 before a reading was recorded.

Oxygen Evolution. Photosynthetic oxygen evolution was measured in a Clark-type oxygen electrode maintained at a constant temperature of 30 °C. The measurements were made in BG-11 containing 25 mM HEPES−NaOH, pH 7.5. Actinic light was provided by a Schott 1500 light source providing 7000 $\mu E \cdot m^{-2} \cdot s^{-1}$ or 700 $\mu E \cdot m^{-2} \cdot s^{-1}$ light passed through a 515 nm cutoff filter. The electron acceptors were 1.0 mM $K_3Fe(CN)_6$ and 0.2 mM 2,5-dimethyl-*p*-benzoquinone. The chlorophyll determinations for oxygen evolution and the other assays in this paper were performed according to MacKinney (*28*).

Quantitation of Photosystem II. Quantitaion of PSII on a chlorophyll basis was estimated through herbicide binding by measuring diuron-replaceable [^{14}C]atrazine binding in whole cells as described in refs (*11*) and (*29*). The specific activity of the [^{14}C]atrazine was 18.6 mCi/mmol, and the chlorophyll concentration was 50 μg mL^{-1}. The samples were incubated for 30 min in the dark with shaking every 10 min.

The relative concentrations of PSII reaction centers were also determined by detecting the variable chlorophyll fluorescence yield in the presence of 20 mM hydroxylamine and 40 μM diuron as described by Nixon and Diner (*30*). The fluorescence yield was measured with an OCCAM Technologies kinetic fluorimeter.

Western Blotting. Thylakoid preparation was performed as described in ref (*31*). However, the centrifugation step prior to ultracentrifuging the samples was performed at 8000*g*. The SDS−PAGE was performed using 12% polyacrylamide gels and the buffer system of Laemmli (*32*) using a BioRad Mini-Protean II, and 5 μg of chlorophyll was loaded for each sample. The proteins were transferred to nitrocellulose using 25 mM Tris, 192 mM glycine, and 20% v/v methanol at pH 8.3, 280 mA, for 45 min (BioRad Mini Trans Blot), and the subsequent Western blots were developed using the BioRad goat anti-rabbit IgG alkaline phosphatase system.

Mutant Construction and Verification. Mutations at charged residues at the beginning of the domain between Gly-351 and Thr-436 in loop E of CP47 were created by using a construct in which *psb*B, lacking the 45 nucleotides that coded for Gly-351 to Thr-365, had been cloned into pUC 19 (*19*). This deletion created an *Eco*RI site into which oligonucleotides with the desired substitutions were inserted. The pair of oligonucleotides used to create G351L/E353Q/E355Q/T365Q were 5′-AATTGCGGCAACTGCAGGTACGGCGTATGCCTAACTTCTTTGAAC-3′ and 5′-AATTGTTCAAAGAAGTTAGGCATACGCCGTACCTGCAGTTGCCGC-3′. The individual nucleotides that have been changed are underlined. The sequence of the appropriate *psb*B clone was confirmed and then used to transform a *psb*B deletion strain

of *Synechocystis* sp. PCC 6803 (*19*). An identical approach was taken to create the strain G351L/E364Q/T365Q. In each case, the insertion of the oligonucleotide pair at the *Eco*RI site introduced the Gly-351 to Leu and Thr-365 to Gln substitutions. To assess the effect of these mutations, the strain G351L/T365Q was also created.

To create the mutant strain Δ(G429-T436) lacking amino acids between Gly-429 and Thr-436 of CP47, the oligonucleotide 5′-GCTCAGTTGGGTGAATTCAACTCTGATG-GT-3′ was synthesized. This mutagenic oligonucleotide was designed to introduce a deletion of 24 nucleotides from nucleotide 1284 from the first codon of *psb*B, thereby creating an *Eco*RI site at position 1281 which has been underlined. After hybridization of the mutagenic oligonucleotide to a *psb*B template that had been cloned into M13mp19, the synthesis of the mutant *psb*B gene was completed in vitro (*19*). Selective degradation of wild-type DNA and propagation of M13mp19 carrying the mutated *psb*B in *Escherichia coli* were performed according to Vermaas et al. (*33*). Subsequently, M13mp19 single-stranded DNA from single clones was sequenced, mutants were identified, and the appropriate mutated *psb*B fragment was excised and cloned into a plasmid containing complementary regions of *psb*B for subsequent homologous recombination. Proper ligation into this plasmid also led to restoration of a complete kanamycin-resistance cartridge, thus providing convenient selection (*19*). The resulting construct isolated from single *E. coli* clones was tested for the expected *psb*B sequence by restriction enzyme digestion prior to transformation of the photoheterotrophic *psb*B deletion strain of *Synechocystis* sp. PCC 6803. The successful creation of the mutant was confirmed by isolation of cyanobacterial genomic DNA by the method of Williams (*27*) and the presence of the mutation confirmed by Southern analysis.

To create the strains E364Q and E364G, the mutagenic oligonucleotides 5′-CCTAACTTCTTTCAGACTTTCCCCG-TC-3′ and 5′-CCTAACTTCTTTGGAACTTTCCCCGTC-3′ were used, respectively, and the nucleotides that were changed in both cases have been underlined. To confirm that the correct mutations were present, *psb*B was obtained by PCR using the forward primer 5′-AATAAAAAT-TAAAACGTCTTTAAGACAC-3′ and the reverse primer 5′-TCCCAAGACTTAGAACCTGTTTGTAAAG-3′. The PCR products for *psb*B were then sequenced with an Applied Biosystems 373A automated DNA sequencer.

For the creation of strains in which the *psb*O gene had been interrupted, the *psb*O gene was amplified by PCR together with an 854 bp piece of flanking downstream DNA that was incorporated to facilitate homologous recombination during the cyanobacterial transformation. The forward primer was 5′-GTTTCGTCCGTGAATTCTGGCTTTGC-TTTC-3′, which contained a synthetic *Eco*RI site for cloning that has been underlined. The reverse primer was 5′-GTAACCAGAGTAGCTCTGCAGTATGAAACC-3′, and contained a synthetic *Pst*I site which has also been underlined. The gene was interrupted at a unique intragenic *Bam*HI site by a 2.0 kb DNA segment conferring spectinomycin resistance (*34*). The resulting PCR product was cloned into pUC 19 and used to transform the control and the strains carrying mutations in *psb*B.

To create mutants which lacked the PSII-V protein, a plasmid, in which a *psb*V intragenic 0.4 kb *Hin*cII-*Xba*I fragment had been replaced by a 1.4 kb erythromycin-resistance cassette from pRL425 from Elhai and Wolk (*35*), was used to transform the *psb*B control and mutant strains. This plasmid is described in Shen et al. (*11*).

To verify that homozygous mutant strains carrying the *psb*O interruption or the *psb*V deletion had been obtained, Southern analysis and PCR analysis were performed. The PCR reaction was carried out on both genomic DNA and single-colony isolates from cyanobacterial cultures. The PCR primers used to demonstrate the deletion of *psb*V corresponded to the forward primer 5′-TGAGAATTGAC-CGATTCCCTTTCTCACCCC-3′ and the reverse primer 5′-CCCTGCCTACCTACCAGGAAATGTTGTTTA-3′. The PCR cycle employed a 3 min 94 °C premelt followed by 30 cycles of 30 s at 92 °C, 2 min at 55 °C, and 3 min at 72 °C. A final extension for 5 min at 72 °C was given at the end of the program. To confirm that the correct *psb*B mutant was present in each of the strains carrying the *psb*O interruption, or the *psb*V deletion, *psb*B was obtained by PCR and sequenced as described for the confirmation of E364Q and E364G.

RESULTS

Location and Construction of psbB Mutations in the Presence and Absence of PSII-O. The ability of PSII-O to support oxygen evolution in the absence of PSII-V and vice versa (*25*) has led us to address the question of whether loop E of CP47 has specific functional requirements in vivo for both PSII-O and PSII-V. This question has been approached by introducing photoautotrophic mutations into loop E of CP47 and characterizing these strains in the presence or absence of either extrinsic protein. The locations of the mutations that have been utilized are within the domain between Gly-351 and Thr-436 of loop E and are shown in Figure 1. Also shown are the regions within loop E that have been reported to interact with the PSII-O protein (*14*−*16*). The three strains initially used were G351L/E353Q/E355Q/T365Q, Δ(R384-V392), and Δ(G429-T436). The construction of G351L/E353Q/E355QT365Q and Δ(G429-T436) has been described under Materials and Methods, and both the control strain and Δ(R384-V392) had been constructed previously (*19*). The control strain possesses a wild-type copy of *psb*B with a kanamycin-resistance cassette located downstream of the *psb*B gene. The phenotype of the control has been shown to be indistinguishable from the wild type with the exception that it is resistant to kanamycin (*19*). To inactivate the *psb*O gene in control, G351L/E353Q/E355Q/T365Q, Δ(R384-V392), and Δ(G429-T436), the *psb*O gene was cloned into pUC 19 as a PCR fragment derived from wild-type genomic DNA. As described under Materials and Methods, the *psb*O gene was then inactivated by the insertion of a 2.0 kb spectinomycin-resistance cassette (*34*) at a *Bam*HI site 558 bp from the beginning of the open reading frame.

The verification of these mutant strains is presented in Figure 2. A restriction map for control, G351L/E353Q/E355Q/T365Q, and Δ(G429-T436) is presented in Figure 2A(i), and Southern hybridization analysis is shown in Figure 2A(ii). The DNA was probed with a *Bst*EII/*Bst*EII 471 bp intragenic fragment. This blot shows that G351L/E353Q/E355Q/T365Q is present as a pure mutant strain as it

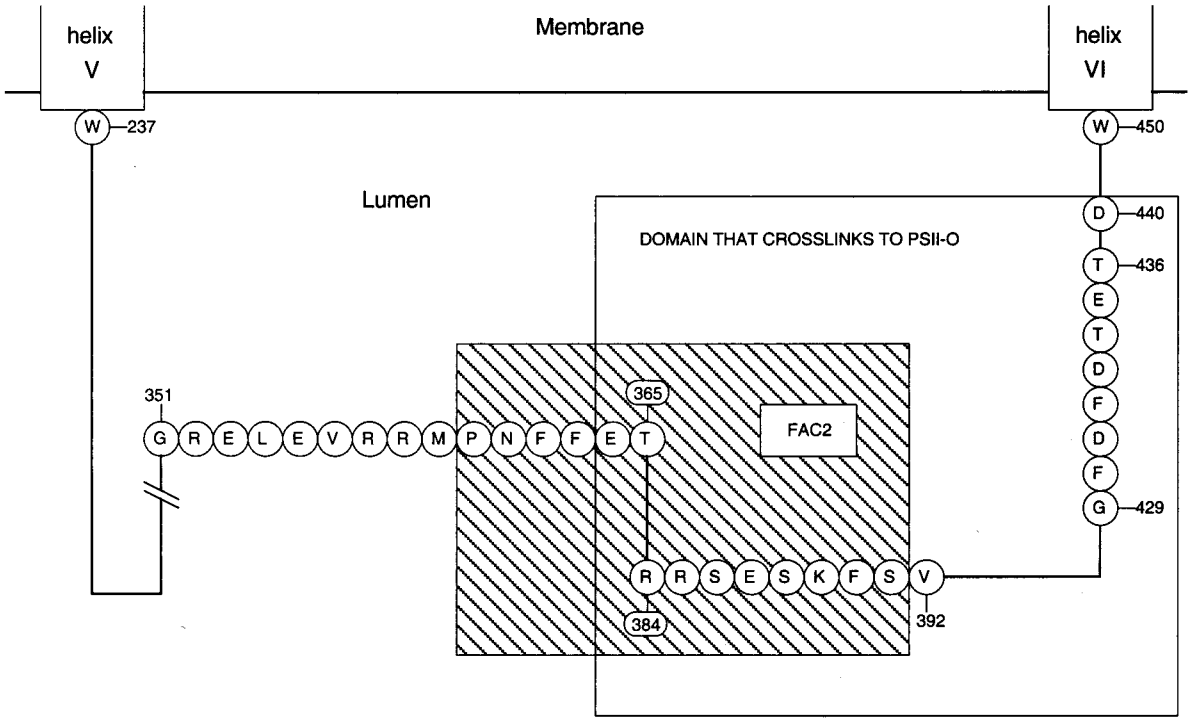

FIGURE 1: Diagram of the large lumen-exposed hydrophilic loop located between helix V and helix VI of CP47. The domain between Glu-364 and Asp-440 that has been shown to cross-link to the N-terminal 76 amino acids of the PSII-O protein is shown by an open box (*14*). The domain from Pro-360 to Ser-391 indicated by the hatched box is an epitope for the monoclonal antibody FAC2 (*15*, *16*). The three regions, Gly-351 to Thr-365, Arg-384 to Val-392, and Gly-429 to Thr-436, that are used in this study to probe interactions with PSII-O and PSII-V, are indicated. The amino acid sequences given are for *Synechocystis* sp. PCC 6803.

resembles the control strain in lane 1 and there is no indication of the presence of the introduced *Eco*RI site used for the insertion of the mutagenic oligonucleotides. Similarly, Δ(G429-T436) is shown to be present as a pure mutant strain with no trace of wild-type DNA. The presence of the *Eco*RI site created by the mutagenic oligonucleotide used for the creation of Δ(G429-T436) was confirmed by comparing the hybridization signals in lane 3 of Figure 2A(ii) with those obtained for the control and G351L/E353Q/E355Q/T365Q in lanes 1 and 2. In the absence of an introduced *Eco*RI site, a single hybridization signal was obtained for an approximately 6.8 kb *Bam*HI/*Bam*HI fragment in the control and G351L/E353Q/E355Q/T365Q strains. In the case of Δ(G429-T436), two *Bam*HI/*Eco*RI fragments were detected in lane 3 at approximately 5.8 and 1.0 kb.

The restriction map corresponding to the introduction of the 2.0 kb spectinomycin-resistance cassette into the *Bam*HI site of *psb*O in control, G351L/E353Q/E355Q/T365Q, Δ-(R384-V392), and Δ(G429-T436) is shown in Figure 2B(i), and Southern hybridization analysis is presented in Figure 2B(ii). The DNA was probed with a 541 bp *Eco*RI/*Bam*HI intragenic fragment obtained from genomic DNA by PCR where the *Eco*RI site had been incorporated into the primer design. Each of the *psb*O-interrupted mutants are present as pure strains with no trace of the corresponding parental *psb*O signal being detected. The *Eco*RI/*Bam*HI probe also recognized a large downstream *Sma*I/*Sma*I fragment which is present as a >12 kb band in all lanes. The new strains were designated as control:ΔPSII-O, G351L/E353Q/E355Q/T365Q:ΔPSII-O, Δ(R384-V392):ΔPSII-O, and Δ(G429-T436):ΔPSII-O. The Western analysis in Figure 2C confirms that interruption of *psb*O resulted in the absence of PSII-O in each of the ΔPSII-O mutants.

Growth Curves in Normal, Calcium-Limiting, and Chloride-Limiting Media. In Figure 3A,B, the photoautotrophic growth curves in normal BG-11 medium are shown for each strain in the presence or absence of the PSII-O protein. The photoautotrophic doubling time for the control and G351L/E353Q/E355Q/T365Q strains was approximately 12 h. Since the oligonucleotides used in the construction of G351L/E353Q/E355Q/T365Q were inserted at an *Eco*RI site, created in *psb*B by removal of the nucleotides that coded for Gly-351 to Thr-365, both the correct orientation and the reversed orientation were possible. Genomic sequencing of the mutant QRM-2 demonstrated that the oligonucleotides had inserted in the reversed direction in this strain, yielding the sequence LFKEVRHTPYLQLPQ between amino acid positions 351 and 365. In Figure 3A, it can be seen that this mutant was unable to grow photoautotrophically.

Both Δ(R384-V392) and Δ(G429-T436) grew photoautotrophically, exhibiting doubling times of 14 and 16 h, respectively. A contrast to this was observed when Δ(R384-V392):ΔPSII-O and Δ(G429-T436):ΔPSII-O were examined. The data in Figure 3B show that Δ(G429-T436):ΔPSII-O was unable to grow while removal of PSII-O in Δ(R384-V392), as well as in the control and G351L/E353Q/E355Q/T365Q, did not prevent photoautotrophic growth. However, removal of PSII-O in Δ(R384-V392):ΔPSII-O extended the doubling time observed for Δ(R384-V392) to 24 h, and similarly in the control:ΔPSII-O and G351L/E353Q/E355Q/T365Q:ΔPSII-O strains, the photoautotrophic doubling times became 24 and 22 h, respectively.

The situation when calcium was omitted from the BG-11 medium by replacing the 0.24 mM $CaCl_2$ with 0.48 mM NaCl is shown in Figure 3C. The four strains that have PSII-O present grow with similar doubling times to those

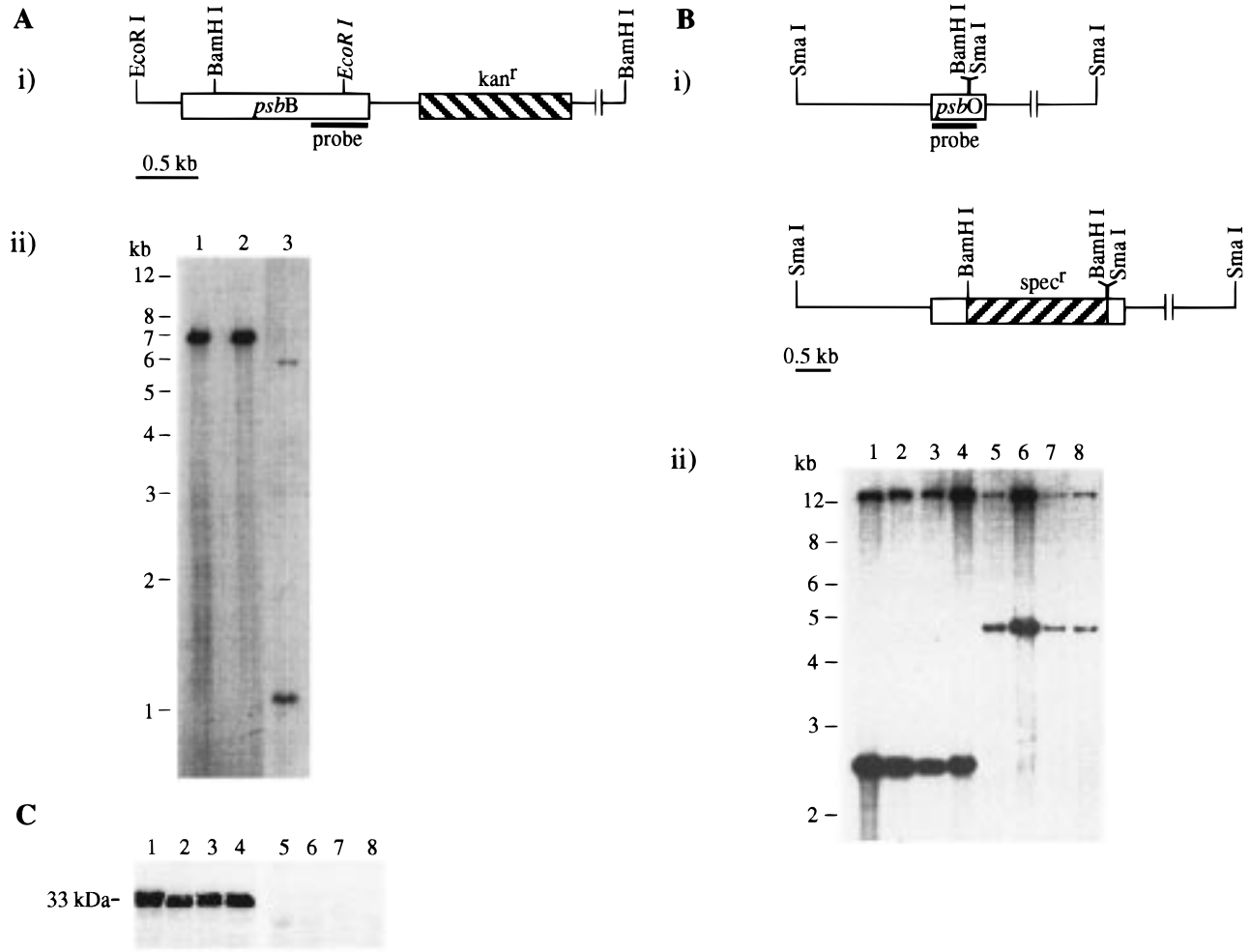

FIGURE 2: (A) (i) Restriction map of the *psb*B region in the *Synechocystis* sp. PCC 6803 genome in control, G351L/E353Q/E355Q/T365Q, and Δ(G429-T436). The *Eco*RI site shown in italics is only present in Δ(G429-T436) (see text for additional details). Each strain contains a 1.2 kb kanamycin-resistance marker (kan^r) inserted at a *Nco*I site 368 nucleotides downstream of *psb*B. (ii) Southern blot of control (lane 1), G351L/E353Q/E355Q/T365Q (lane 2), and Δ(G429-T436) (lane 3). *Synechocystis* sp. PCC 6803 DNA was cut with *Bam*HI and *Eco*RI and probed with a 471 bp intragenic *Bst*EII/*Bst*EII fragment. (B) (i) Restriction maps of the *psb*O region and flanking DNA between two *Sma*I sites in the *Synechocystis* sp. PCC 6803 genome with or without the insertion of a 2.0 kb spectinomycin-resistance marker (spec^r) inserted at a *Bam*HI site 558 bp from the initial base of the start codon. (ii) Southern blot of control (lane 1), G351L/E353Q/E355Q/T365Q (lane 2), Δ(R384-V392) (lane 3), Δ(G429-T436) (lane 4), and their corresponding strains with an inactivated *psb*O gene containing the 2.0 kb spectinomycin-resistance marker (lanes 5−8). The *Synechocystis* sp. PCC 6803 genomic DNA was cut with *Sma*I and probed with a PCR-generated 540 bp *Eco*RI/*Bam*HI intragenic fragment. The synthetic *Eco*RI site was introduced at nucleotide 17 from the initial base of the start codon. (C) Western blot of *Synechocystis* sp. PCC 6803 thylakoid membranes probed with an antibody raised against the spinach PSII-O protein. Control (lane 1), G351L/E353Q/E355Q/T365Q (lane 2), Δ(R384-V392) (lane 3), Δ(G429-T436) (lane 4), control: ΔPSII-O (lane 5), G351L/E353Q/E355Q/T365Q:ΔPSII-O (lane 6), Δ(R384-V392):ΔPSII-O (lane 7), and Δ(G429-T436):ΔPSII-O (lane 8).

obtained in normal BG-11 medium, but no strains could grow when PSII-O was absent. This result has been seen before for wild type with the *psb*O gene interrupted or deleted (*22*, *36*). Figure 3C therefore supports the conclusion that the PSII-O protein is functionally associated with all three strains carrying mutations between Gly-351 and Thr-436. The concentration of calcium in the calcium-limiting BG-11 medium was determined to be less than 0.1 μM by atomic emission of the inductively coupled plasma (*37*).

The effect of omitting chloride in the BG-11 medium was also examined (data not shown). In this experiment, $MnSO_4$ replaced $MnCl_2$, and $Ca(NO_3)_2$ replaced $CaCl_2$. This reduced the chloride concentration in the BG-11 medium from 0.48 mM to a level that could not be detected by titration with sodium borohydride (*38*). When chloride was omitted, the photoautotrophic doubling times for the control and G351L/E353Q/E355Q/T365Q were extended to approximately 16 h each. The effect on Δ(R384-V392) was more pronounced, and the doubling time for this strain increased to 44 h while Δ(G429-T436) was completely inhibited and all strains lacking the PSII-O protein were unable to grow photoautotrophically under these conditions. In addition, all strains, irrespective of the presence or absence of PSII-O, were able to grow in the presence of 20 μM diuron and 5 mM glucose with a photoheterotrophic doubling time of approximately 22 h in the chloride-limiting medium, and the doubling time for the control strain, in the presence of chloride, was also 22 h under these photoheterotrophic conditions. This result confirms that the effect of chloride is located in PSII.

Determination of the Levels of PSII in the Presence and Absence of PSII-O. To address the levels of PSII assembled in the different strains, herbicide-binding assays were performed with different concentrations of radiolabeled atrazine, a PSII-directed herbicide. The data are presented

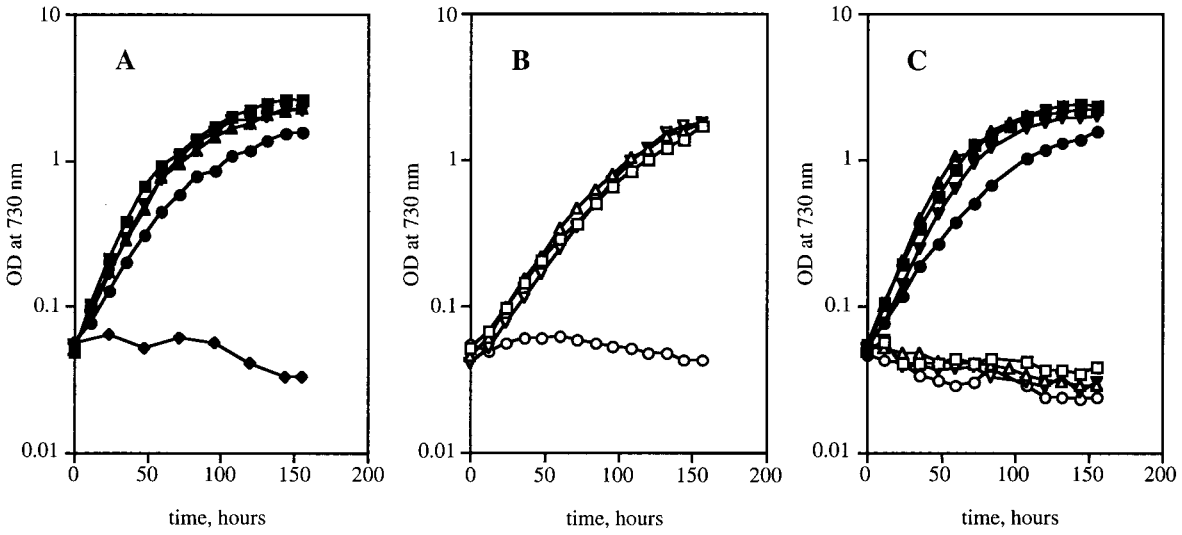

FIGURE 3: Photoautotrophic growth of *Synechocystis* sp. PCC 6803 strains as measured by the optical density at 730 nm in BG-11 medium (A and B) and in calcium-limiting BG-11 (C). (A) Control (■), G351L/E353Q/E355Q/T365Q (▲), Δ(R384-V392) (▼), Δ(G429-T436) (●), and QRM-2 (◆). (B) Control:ΔPSII-O (□), G351L/E353Q/E355Q/T365Q:ΔPSII-O (△), Δ(R384-V392):ΔPSII-O (▽), and Δ(G429-T436):ΔPSII-O (○). (C) Control (■), G351L/E353Q/E355Q/T365Q (▲), Δ(R384-V392) (▼), and Δ(G429-T436) (●). Open symbols correspond to strains without PSII-O.

Table 1: Chlorophyll per PSII Reaction Center (Chl/PSII) and Atrazine Affinity (K_d = Dissociation Constant)

strain	Chl/PSII	K_d (nM)
control	740	250
G351L/E353Q/E355Q/T365Q	740	270
Δ(R384-V392)	1300	250
Δ(G429-T436)	1950	230
control:ΔPSII-O	1210	250
G351L/E353Q/E355Q/T365Q:ΔPSII-O	1210	250
Δ(R384-V392):ΔPSII-O	1310	250
Δ(G429-T436):ΔPSII-O	ND[a]	ND[a]

[a] ND = no measurable [^{14}C]atrazine binding could be detected.

in Table 1. The number of PSII centers present in G351L/E353Q/E355Q/T365Q was unchanged from that detected in the control strain. A Chl/PSII ratio of 740 was obtained for both cultures. In contrast, Δ(R384-V392) was found to have a PSII/Chl ratio of 1300, suggesting that there was a 50% reduction of PSII centers in this strain. The number of PSII centers was reduced further in Δ(G429-T436) with the Chl/PSII ratio becoming 1950. In a previous study, the ratio of Chl/PSII for Δ(R384-V392) had been determined to be 1700 (*19*). The variation seen between the two measurements of the same strain highlights the strict requirement for identical growth conditions to be maintained for different experiments.

The effect of removing the PSII-O protein was found to increase the Chl/PSII ratio to approximately 1210 for both the control:ΔPSII-O and G351L/E353Q/E355Q/T365Q:ΔPSII-O strains, but the Chl/PSII ratio for Δ(R384-V392) was found to be virtually unchanged by the removal of PSII-O with the Chl/PSII-O ratio for Δ(R384-V392):ΔPSII-O determined to be 1310. In contrast, the effect of creating the strain Δ(G429-T436):ΔPSII-O was to destabilize PSII such that no centers could be detected in the assay.

The relative levels of assembled PSII reaction centers were also determined by measuring the variable chlorophyll fluorescence yield from PSII (*30*). A good correspondence has been shown between measurements of variable chlorophyll fluorescence yield and herbicide-bindings assays that are performed on the same samples [e.g., (*39*, *40*)]. In the case of the control:ΔPSII-O strain, the measured variable chlorophyll fluorescence yield indicated the presence of about 75% of the functional PSII centers found in the control while our herbicide-binding data indicated a relative concentration of PSII centers of about 60% of the control. These numbers are similar to those previously determined for a *psb*O interruption mutant by measurement of the variable chlorophyll fluorescence yield where the relative concentration of PSII was 60−90% of the number of wild-type PSII centers (*22*). In the case of Δ(G429-T436):ΔPSII-O, no variable chlorophyll fluorescence yield was detected, supporting the interpretation that PSII was not assembled in this strain (data not shown).

To further explore the phenotype of the different mutant strains, oxygen evolution from whole cells was measured with a Clark electrode and is presented for two different light intensities in Figure 4. At an actinic light intensity of 7000 $\mu E \cdot m^{-2} \cdot s^{-1}$, both the control strain and G351L/E353Q/E355Q/T365Q were able to maintain a relatively stable rate of oxygen evolution, but Δ(R384-V392) and Δ(G429-T436) became fully photoinactivated under constant illumination (Figure 4A). Interestingly, Δ(G429-T436) exhibited a higher initial rate of oxygen evolution than Δ(R384-V392) even though the results in Table 1 demonstrate that Δ(G429-T436) had fewer detectable PSII centers. Therefore, Δ(R384-V392) appears to introduce a lesion in PSII activity. The initial rate for Δ(G429-T436) was 60% of the control rate and became fully inhibited in 3.5 min while the initial rate for Δ(R384-V392) was 36% of the control rate and was reduced to zero in 2.5 min. In contrast, the data shown in Figure 4B show that at 700 $\mu E \cdot m^{-2} \cdot s^{-1}$ both of these strains were able to produce stable rates of oxygen evolution of approximately 38% those observed for the control at high light while the control and G351L/E353Q/E355Q/T365Q strains at 700 $\mu E \cdot m^{-2} \cdot s^{-1}$ exhibited oxygen evolution rates of approximately 70% of those obtained initially at 7000 $\mu E \cdot m^{-2} \cdot s^{-1}$ (data not shown).

In Figure 4C,D, the oxygen evolution data are presented for the strains that have the *psb*O gene interrupted. In the

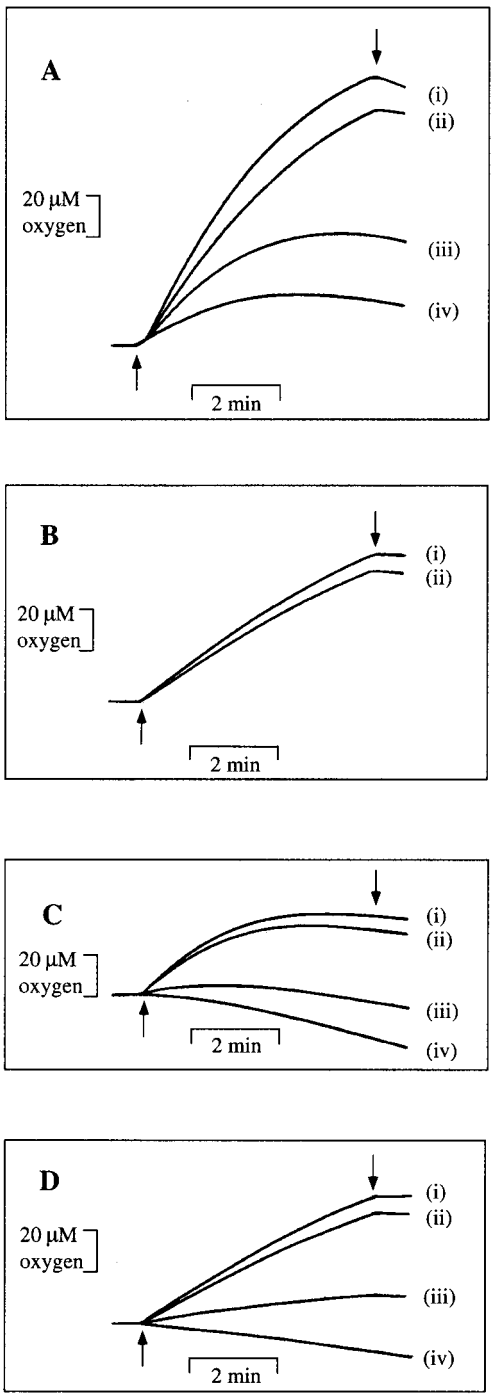

FIGURE 4: Traces of oxygen concentration from cells of *Synechocystis* sp. PCC 6803 determined polarographically with a Clark electrode. The 3 mL reaction chamber held cell suspensions containing 10 μg of chlorophyll/mL. Samples were illuminated with yellow light at either 7000 $\mu E \cdot m^{-2} \cdot s^{-1}$ (A and C) or 700 $\mu E \cdot m^{-2} \cdot s^{-1}$ (B and D). The arrows indicate when the light was turned on and off. (A) (i) Control; (ii) G351L/E353Q/E355Q/T365Q; (iii) Δ(G429-T436), and (iv) Δ(R384-V392). (B) (i) Δ(G429-T436) and (ii) Δ-(R384-V392). (C and D) (i) Control:ΔPSII-O; (ii) G351L/E353Q/E355Q/T365Q:ΔPSII-O; (iii) Δ(R384-V392):ΔPSII-O; and (iv) Δ(G429-T436):ΔPSII-O. The initial rate of oxygen evolution for the control strain in panel A was 264 μmol of $O_2 \cdot$(mg of Chl)$^{-1} \cdot h^{-1}$.

control and G351L/E353Q/E355Q/T365Q, the removal of the PSII-O protein introduces a clear susceptibility to photoinactivation which is removed at 700 $\mu E \cdot m^{-2} \cdot s^{-1}$. A similar result has been observed for wild type carrying a deleted or interrupted *psb*O gene (*22*). In the absence of PSII-O, neither Δ(R384-V392) nor Δ(G429-T436) evolved oxygen at 7000 $\mu E \cdot m^{-2} \cdot s^{-1}$. However, at 700 $\mu E \cdot m^{-2} \cdot s^{-1}$, Δ(R384-V392):ΔPSII-O was able to produce a small stable rate of approximately 10% of the initial rate measured for the control strain in Figure 4A. From a comparison of Figure 4B(ii) with Figure 4D(iii), it can be seen that, at 700 $\mu E \cdot m^{-2} \cdot s^{-1}$, the removal of PSII-O in Δ(R384-V392):ΔPSII-O introduced an additional inhibition of PSII oxygen evolution even though the number of assembled PSII centers detected in both Δ(R384-V392) and Δ(R384-V392):ΔPSII-O was similar. The control:ΔPSII-O strain evolved oxygen at 50% the rate of the control strain at 700 $\mu E \cdot m^{-2} \cdot s^{-1}$ in agreement with earlier reports (*21*, *22*), and a similar result was obtained with G351L/E353Q/E355Q/T365Q in the presence and in the absence of PSII-O. In the case of Δ-(G429-T436):ΔPSII-O, no oxygen evolution was detected, consistent with PSII not being assembled in this strain. In fact, in both high and low light, an oxygen consumption was measured for Δ(G429-T436):ΔPSII-O. The origin of this uptake was not investigated in this study.

Construction and Characterization of Mutant Strains Lacking PSII-V. To remove the PSII-V protein, the control, G351L/E353Q/E355Q/T365Q, Δ(R384-V392), and Δ(G429-T436) strains were each transformed with a plasmid in which the portion of *psb*V between a *Hinc*II site at position 81 and an *Xba*I site at position 479 had been replaced by a 1.4 kb erythromycin-resistance cassette (*11*). The *psb*V gene is 483 bp in length. In Figure 5A, the photoautotrophic growth curves for the control, G351L/E353Q/E355Q/T365Q, Δ-(R384-V392), and Δ(G429-T436), in which PSII-V had been deleted, are presented. The control:ΔPSII-V and G351L/E353Q/E355Q/T365Q:ΔPSII-V exhibited photoautotrophic doubling times of 17 and 22 h, respectively. However, both Δ(R384-V392):ΔPSII-V and Δ(G429-T436):ΔPSII-V were unable to support photoautotrophic growth. This result demonstrated that the strain Δ(R384-V392) required the presence of PSII-V for photoautotrophic growth while the removal of PSII-O had had a negligible impact. In addition, no strains lacking PSII-V were able to grow in either the calcium-limiting or the chloride-limiting media (data not shown). Therefore, under the stress conditions induced by omitting either of these ions, the presence of either PSII-O or PSII-V, in the absence of the other, was no longer sufficient to support photoautotrophic growth.

To verify the identity of each strain in Figure 5A and demonstrate that *psb*V had been deleted, the genomic DNA was isolated, *psb*B was sequenced, and a PCR reaction was performed using primers for *psb*V. The result of colony PCR on all strains is shown in Figure 5B and demonstrates that *psb*V has been removed and replaced by the 1.4 kb erythromycin-resistance cassette, resulting in an approximately 0.92 kb increase in the PCR product for the strains lacking *psb*V. There was no trace of *psb*V in any mutants, confirming that all strains were homozygous for the deletion.

To investigate whether PSII had assembled in the mutants lacking PSII-V, herbicide-binding assays were performed. The data in Figure 5C demonstrate that the effect of the removal of PSII-V from both the control and G351L/E353Q/E355Q/T365Q was to increase the Chl/PSII ratio to approximately 1000. The Chl/PSII ratio for the control in this experiment was 670 (data not shown). In addition, the dissociation constant for atrazine binding appeared to increase

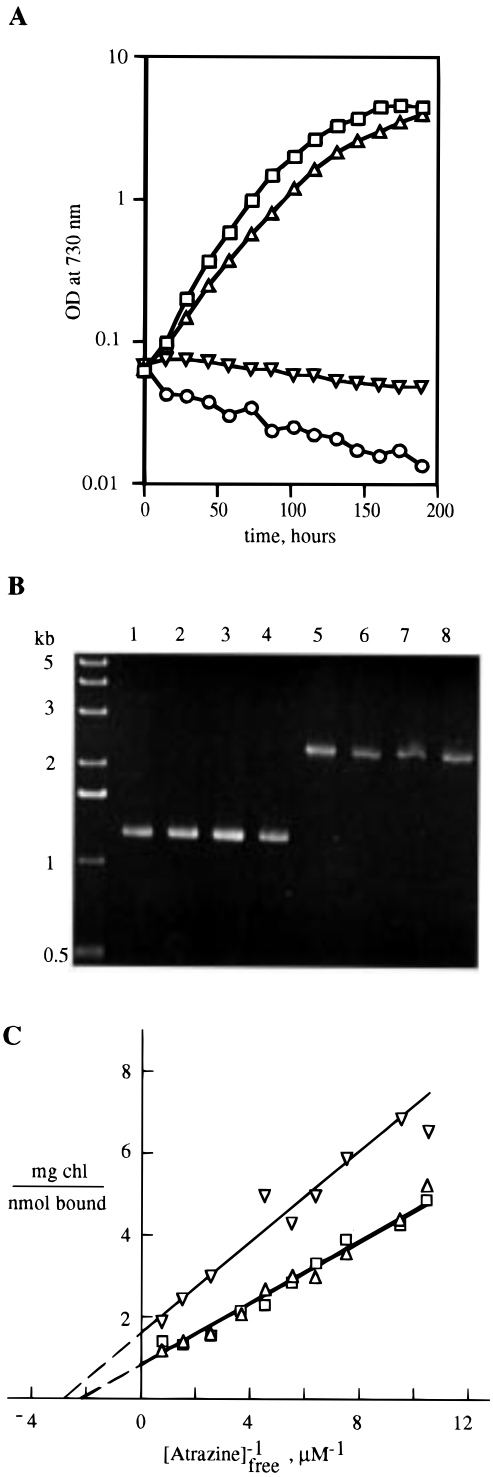

FIGURE 5: (A) Photoautotrophic growth of *Synechocystis* sp. PCC 6803 strains as measured by the optical density at 730 nm. Control: ΔPSII-V (□), G351L/E353Q/E355Q/T365Q:ΔPSII-V (△), Δ(R384-V392):ΔPSII-V (▽), and Δ(G429-T436):ΔPSII-V (○). (B) PCR amplification of *Synechocystis* sp. PCC 6803 genomic DNA with primers flanking the *psb*V gene. Lane 1, control; lane 2, G351L/E353Q/E355Q/T365Q; lane 3, Δ(R384-V392); lane 4, Δ(G429-T436); lane 5, control:ΔPSII-V; lane 6, G351L/E353Q/E355Q/T365Q:ΔPSII-V; lane 7, Δ(R384-V392):ΔPSII-V; and lane 8, Δ(G429-T436):ΔPSII-V. The marker lane is a 1 kb ladder supplied by GIBCOBRL Life Technologies. (C) Atrazine-binding assays of *Synechocystis* sp. PCC 6803 strains lacking the PSII-V protein. Control:ΔPSII-V (□), G351L/E353Q/E355Q/T365Q:ΔPSII-V (△), and Δ(R384-V392):ΔPSII-V (▽).

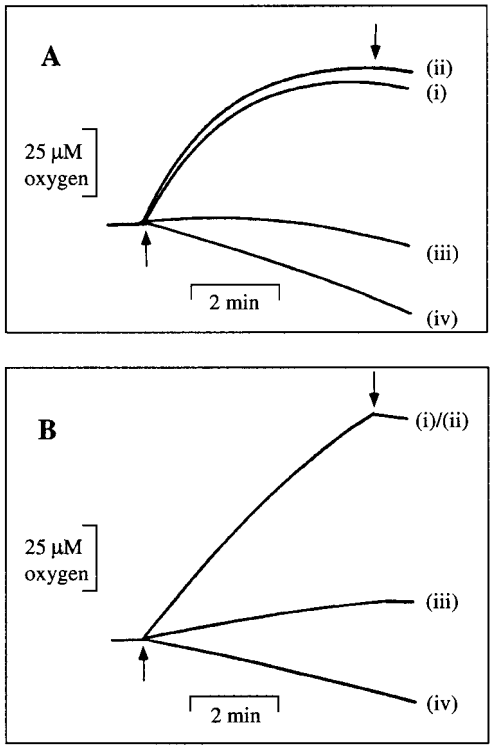

FIGURE 6: Traces of oxygen concentration from *Synechocystis* sp. PCC 6803 strains that lack the PSII-V protein determined polarographically with a Clark electrode. The 3 mL reaction chamber held cell suspensions containing 10 μg of chlorophyll/mL. Samples were illuminated with yellow light at 7000 $\mu E \cdot m^{-2} \cdot s^{-1}$ in panel A and at 700 $\mu E \cdot m^{-2} \cdot s^{-1}$ in panel B. The arrows indicate when the light was turned on and off. (i) Control:ΔPSII-V; (ii) G351L/E353Q/E355Q/T365Q:ΔPSII-V; (iii) Δ(R384-V392):ΔPSII-V; and (iv) Δ(G429-T436):ΔPSII-V.

in the absence of PSII-V from approximately the 250 nM value in Table 1 to approximately 380 nM in Figure 5C. A similar decrease in the affinity of the binding for atrazine is evident in the data obtained for the wild type measured in the absence of PSII-V (*11*). In the case of Δ(R384-V392):ΔPSII-V, the Chl/PSII ratio was found to be 1790. These data indicate that, relative to the control strain, the removal of PSII-V in the control and G351L/E353Q/E355Q/T365Q resulted in a 33% reduction of PSII centers while a reduction of 63% was observed in Δ(R384-V392):ΔPSII-V. There was no detectable herbicide binding in Δ(G429-T436):ΔPSII, indicating that PSII does not assemble in this mutant and no variable chlorophyll fluorescence yield could be detected (data not shown).

To complete the phenotypic analysis, oxygen evolution was measured in the PSII-V minus mutants and is presented in Figure 6. At 7000 $\mu E \cdot m^{-2} \cdot s^{-1}$, Δ(R384-V392):ΔPSII-V was unable to evolve oxygen, and no oxygen evolution was detected for Δ(G429-T436):ΔPSII-V either at 7000 $\mu E \cdot m^{-2} \cdot s^{-1}$ or at 700 $\mu E \cdot m^{-2} \cdot s^{-1}$. However, at 700 $\mu E \cdot m^{-2} \cdot s^{-1}$, a slight rate was seen for Δ(R384-V392):ΔPSII-V, consistent with the quantitation of assembled PSII. The origin of the oxygen uptake detected in Figure 6 for Δ(G429-T436):ΔPSII-V was again not investigated. The removal of PSII-V appeared to make both the control and G351L/E353Q/E355Q/T365Q less susceptible to photoinactivation than the removal of PSII-O. This can be seen from comparing the oxygen evolution traces in Figure 4C and Figure 6A. However, at 7000 $\mu E \cdot m^{-2} \cdot s^{-1}$, both control:ΔPSII-V and G351L/E353Q/E355Q/

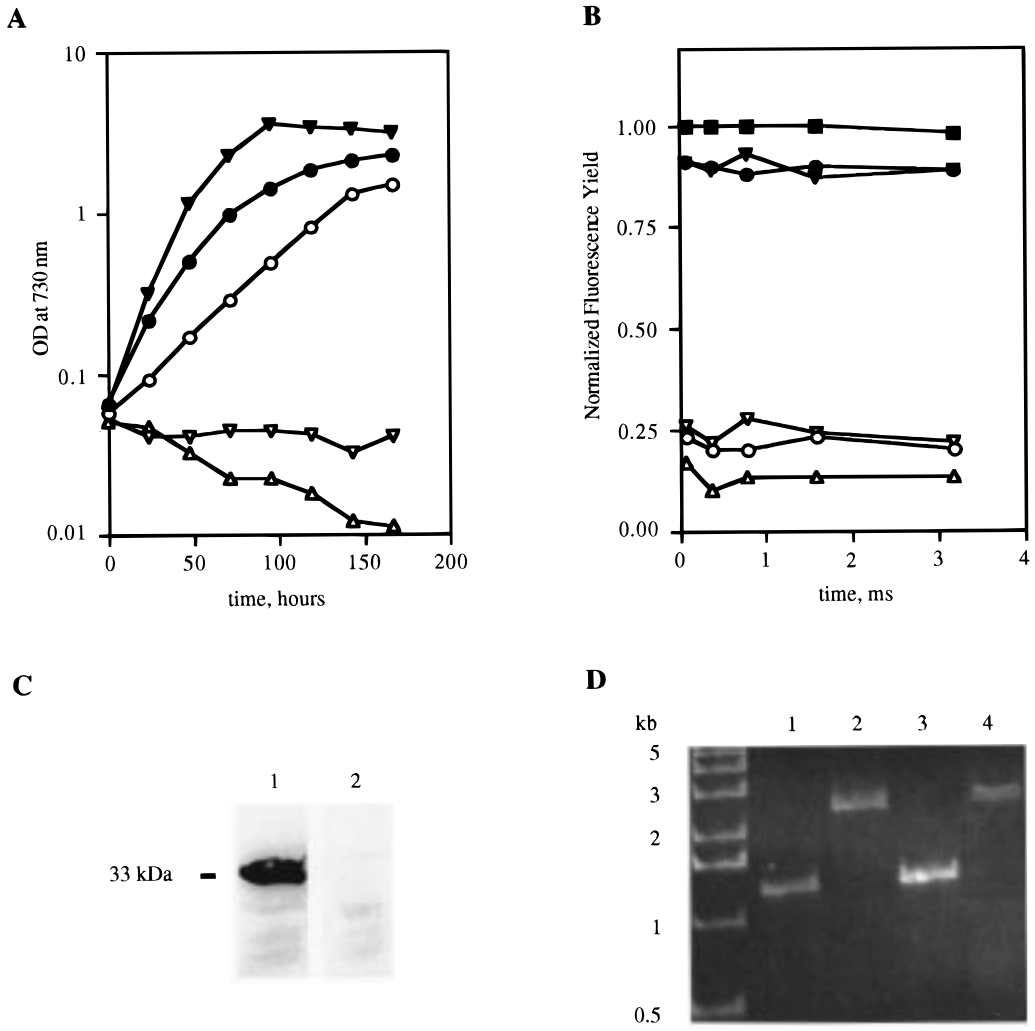

FIGURE 7: (A) Photoautotrophic growth of *Synechocystis* sp. PCC 6803 strains as measured by the optical density at 730 nm. G351L/E364Q/T365Q (●), E364Q (▼), G351L/E364Q/T365Q:ΔPSII-O (○), G351L/E364Q/T365Q:ΔPSII-V (△), and E364Q:ΔPSII-V (▽). (B) The ratio of the normalized fluorescence yield for each mutant, $((F - F_o)/F_o)_M$, to the normalized fluorescence yield of the control, $((F - F_o)/F_o)_{CON}$, which provides an approximate measure of the relative amount of photochemically intact PSII complexes in each strain. F is the fluorescence yield determined at the specified times after a series of 15 actinic flashes spaced at 10 Hz, and F_o is the initial fluorescence yield measured in the dark-adapted sample. Control (■), G351L/E364Q/T365Q (●), E364Q (▼), G351L/E364Q/T365Q:ΔPSII-O (○), G351L/E364Q/T365Q:ΔPSII-V (△), and E364Q:ΔPSII-V (▽). (C) Western blot of *Synechocystis* sp. PCC 6803 thylakoid membranes probed with an antibody raised against the spinach PSII-O protein. Lane 1, G351L/E364Q/T365Q; and lane 2, G351L/E364Q/T365Q:ΔPSII-O. (D) PCR amplification of *Synechocystis* sp. PCC 6803 genomic DNA with primers flanking the *psb*V gene. Lane 1, G351L/E364Q/T365Q; lane 2, G351L/E364Q/T365Q:ΔPSII-V; lane 3, E364Q; and lane 4, E364Q:ΔPSII-V. The marker lane is a 1 kb ladder supplied by GIBCOBRL Life Technologies.

T365Q:ΔPSII-V were photoinactivated with a half-time of approximately 2 min. In contrast, in Figure 6B, a stable oxygen evolution rate of 135 μmol of O_2·(mg of Chl)$^{-1}$·h^{-1} was measured for both the control:ΔPSII-V and G351L/E353Q/E355Q/T365Q:ΔPSII-V at 700 μE·m^{-2}·s^{-1}. This rate is approximately 72% of the initial rate observed for the control at 7000 μE·m^{-2}·s^{-1}.

Characterization of the Mutant Strain G351L/E364Q/T365Q. The sensitivity of Δ(R384-V392) to the removal of PSII-V led us to consider the significance of Glu-364 in CP47 which is located in the same region of loop E as the deletion in Δ(R384-V392). Figure 1 indicates that these amino acids are located within the epitope that is recognized by the monoclonal antibody FAC2 (*15*, *16*). To construct the mutant strain G351L/E364Q/E365Q and the strain G351L/E365Q, which was designed to control for the mutations introduced at Gly-351 and Thr-365 by the insertion of the oligonucleotides at the introduced *Eco*RI site, corresponding mutagenic oligonucleotide pairs were synthesized and incorporated into *psb*B as described under Materials and Methods. The verification of these mutant strains was performed by sequencing of the *psb*B gene from each mutant and by demonstrating the loss of the introduced *Eco*RI site by digestion of the corresponding PCR products with *Eco*RI (data not shown). The phenotypes of G351L/T365Q and the G351L/T365Q strains lacking either PSII-O or PSII-V were similar to those reported here for the corresponding control and G351L/E353Q/E355Q/T365Q strains and will not be considered further.

The characterization of G351L/E364Q/T365Q, G351L/E364Q/T365Q:ΔPSII-O, and G351L/E364Q/T365Q:ΔPSII-V is shown in Figure 7 and Table 2. The photoautotrophic doubling time observed for G351L/E364Q/E365Q in Figure 7A was 14 h. There was no significant effect on the photoautotrophic growth rate of this strain in BG-11 media in which either calcium or chloride had been omitted when

Table 2: Relative Rates of Oxygen Evolution in Strains Carrying Mutations at Glu-364 in CP47

strain	$VO_{2,\ max}$[a] high light	$VO_{2,\ max}$[a] low light
control	100	100
G351L/E364Q/T365Q	85	79
G351L/E364Q/T365Q:ΔPSII-O	ND[b]	24
G351L/E364Q/T365Q:ΔPSII-V	ND[b]	20
E364Q	91	95
E364Q:ΔPSII-V	39[c]	50
E364G	82	83
E364G:ΔPSII-V	34[c]	44

[a] Maximal rate of O_2 evolution ($VO_{2,\ max}$) expressed as a percentage of the rate observed for the control. The average control rate (100%) was determined to be 330 μmol of O_2·(mg of Chl)$^{-1}$·h^{-1} at 7000 μE·m^{-2}·s^{-1} (high light) and 200 μmol of O_2·(mg of Chl)$^{-1}$·h^{-1} at 700 μE·m^{-2}·s^{-1} (low light). The sample was measured at a concentration of 10 μg of chlorophyll·mL^{-1}. [b] No oxygen evolution was detected in these strains. [c] The observed rate was unstable and fully inactivated in <2 min.

the photoautotrophic growth was compared with that of the control strain (data not shown). However, in normal BG-11, the removal of PSII-O in G351L/E364Q/E365Q:ΔPSII-O extended the photoautotrophic doubling time to 31 h, and, strikingly, the strain G351L/E364Q/T365Q:ΔPSII-V was unable to support photoautotrophic growth.

To assess the relative levels of PSII assembled in these strains, herbicide-binding assays were performed. The Chl/PSII ratio for G351L/E364Q/E365Q was found to be similar to that of the control strain, but no reliable herbicide binding was detected for either G351L/E364Q/T365Q:ΔPSII-O or G351L/E364Q/T365Q:ΔPSII-V due to the accuracy of this assay when too few centers are present (data not shown). The results in Figure 7B, however, show the relative levels of PSII reaction centers detected in all three strains by measuring the variable chlorophyll fluorescence yield. In the case of G351L/E364Q/T365Q, the relative level of assembled PSII was 0.90, when compared to the control, while the relative levels of assembled PSII reaction centers in G351L/E364Q/T365Q:ΔPSII-O and G351L/E364Q/T365Q:ΔPSII-V were 0.21 and 0.13, respectively.

The confirmation that PSII-O is absent in G351L/E364Q/T365Q:ΔPSII-O and that *psb*V has been deleted in G351L/E364Q/T365Q:ΔPSII-V is also presented in Figure 7. Figure 7C shows the complete absence of the PSII-O protein as determined by Western blotting analysis, and the PCR result in Figure 7D shows the replacement of *psb*V with the 1.4 kb gene conferring erythromycin resistance in the strain G351L/E364Q/T365Q:ΔPSII-V. The relative rates of oxygen evolution for these strains are presented in Table 2. At 7000 μE·m^{-2}·s^{-1}, G351L/E364Q/T365Q exhibited an initial rate of oxygen evolution that was 85% of the control strain, but G351L/E364Q/T365Q:ΔPSII-O and G351L/E364Q/T365Q:ΔPSII-V were rapidly photoinactivated. When an actinic light intensity of 700 μE·m^{-2}·s^{-1} was used, the initial rate of oxygen evolution for G351L/E364Q/T365Q was found to be 79% of the rate observed for the control under these conditions, and in agreement with the presence of functional PSII centers detected in Figure 7B, a stable rate of 48 μmol of O_2·(mg of Chl)$^{-1}$·h^{-1} was observed in the case of G351L/E364Q/T365Q:ΔPSII-O and a rate of 39 μmol of O_2·(mg of Chl)$^{-1}$·h^{-1} was measured for G351L/E364Q/T365Q:ΔPSII-V.

Confirmation That Substitutions at Glu-364 Prevent Photoautotrophic Growth in the Absence of PSII-V. From the above results, the mutation of Glu-364 to Gln in G351L/E364Q/T365Q:ΔPSII-V appears to be responsible for the inability of this strain to grow photoautotrophically. To confirm the importance of Glu-364, and to determine if the presence of the mutations at Gly-351 and Thr-365 contributes to the observed inhibition, the strains E364Q and E364Q:ΔPSII-V were created (see Materials and Methods). The result in Figure 7A demonstrates that E364Q had a photoautotrophic doubling time of 10 h but E364Q:ΔPSII-V was unable to support photosynthesis. In Figure 7B, the relative levels of assembled PSII reaction centers in E364Q and E364Q:ΔPSII-V were 0.9 and 0.24, respectively, and the homozygous replacement of *psb*V with the erythromycin-resistance cassette in E364Q:ΔPSII-V was confirmed in Figure 7D. Similar results were obtained for the strains E364G and E364G:ΔPSII-V (data not shown).

The relative rates of oxygen evolution for these strains are shown in Table 2. The combined data in Figure 7 and Table 2 suggest that the presence of Gly-351 and/or Thr-365 further destabilizes PSII in the presence of Gln at position 364. A herbicide-binding assay was also performed on E364Q and E364Q:ΔPSII-V. Both the control and E364Q had a Chl/PSII ratio of 560 while the Chl/PSII ratio in E364Q:ΔPSII-V was found to be 1790 (data not shown). This result indicates that there are more assembled PSII reaction centers in E364Q:ΔPSII-V than in G351L/E364Q/T364Q:ΔPSII-V. However, despite its rate of approximately 100 μmol of O_2·(mg of Chl)$^{-1}$·h^{-1} at 700 μE·m^{-2}·s^{-1}, the strain E364Q:ΔPSII-V was unable to support photoautotrophic growth (cf. Figure 7A) and a similar result was obtained with E364G:ΔPSII-V. It is possible that both the function and assembly of PSII are impaired to such a degree in strains possessing mutations at Glu-364 in the absence of PSII-V that the incorporation of new PSII centers into the thylakoid membrane is unable to keep up with the rate of photoinhibitory damage occurring during photoautotrophic growth. However, the experimental results reported here do not directly address this issue.

DISCUSSION

The Different Dependencies on PSII-O and PSII-V. Different domains of loop E of CP47 respond differently to the removal of the extrinsic proteins PSII-O and PSII-V. This is illustrated by the two strains Δ(R384-V392) and Δ(G429-T436). The deletion between Arg-384 and Val-392 was selected because it is found in the epitope for the monoclonal antibody FAC2 (*15*, *16*). The choice of the deletion between Gly-429 and Thr-436 was made because this is located in a region of loop E that had not been investigated in the deletion map constructed by Eaton-Rye and Vermaas (*19*) and Haag et al. (*39*) and it was also located at the N-terminal end of the Glu-364 to Asp-440 domain that is closely associated with the 76 N-terminal amino acids of PSII-O (*14*). Interruption of *psb*O in Δ(G429-T436) created an obligate photoheterotrophic mutant in which functional PSII centers could not be detected, suggesting a requirement for PSII-O in the stable assembly of the PSII complex in this strain. The amino acid sequences for the regions where mutations have been introduced are presented for all species available in the GenEMBL database in Figure 8. A consideration of

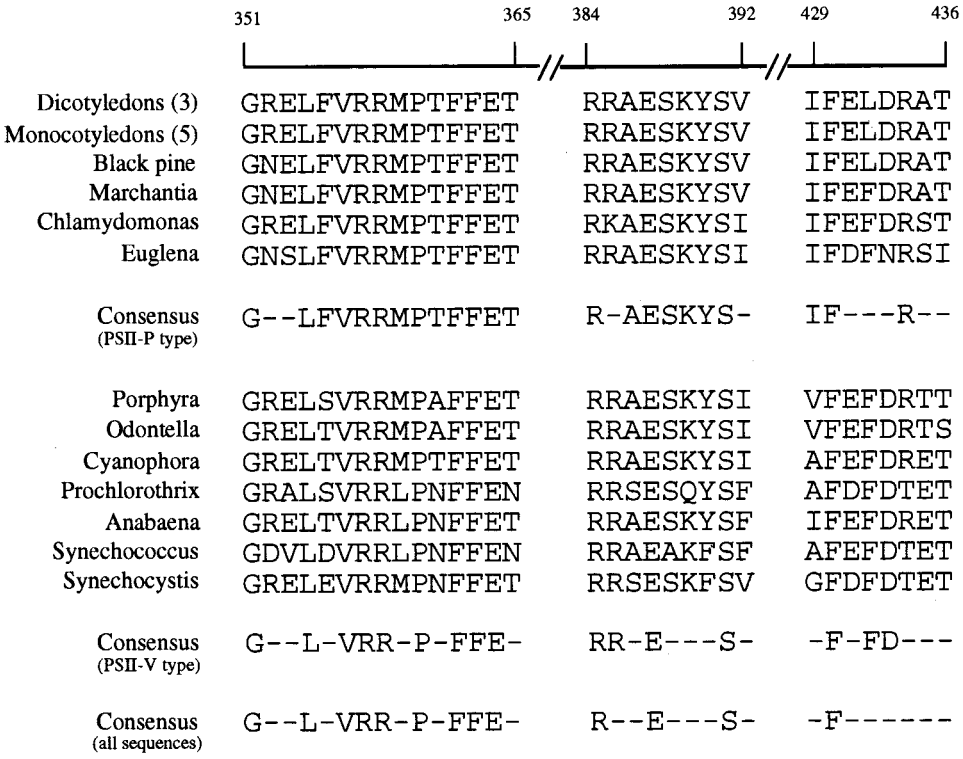

FIGURE 8: Alignment of CP47 sequences obtained from the GenEMBL database using the GCG software package (*54*, *55*). The dicotyledons are *Oenothera hookeri* (Accession No. X55900), *Spinacia oleracea* (Accession No. X02945, X00471), and *Nicotiana tabacum* (Accession No. Z00044, S54304). The monocotyledons are *Hordeum vulgare* (Accession No. X14107), *Oryza sativa* (Accession No. X15901), *Secale cereale* (Accession No. X07672), *Triticum aestivum* (Accession No. X54749), and *Zea mays* (Accession No. X05422). The other species are *Pinus thunbergiana* (Accession No. D17510), *Marchantia polymorpha* (Accession No. X04465, Y00686), *Chlamydomonas reinhardtii* (Accession No. M84022), *Euglena gracilis* (Accession No. X15903, S55899), *Porphyra purpurea* (Accession No. U38804), *Odontella sinensis* (Accession No. Z67753), *Cyanophora paradoxa* (Accession No. U30821), *Prochlorothrix hollandica* (Accession No. X59614), *Anabaena* sp. PCC 7120 (Accession No. X58847), *Synechococcus* sp. PCC 7942 (Accession No. Z14087), and *Synechocystis* sp. PCC 6803 (Accession No. M17109).

the sequence between Gly-429 and Thr-436 reveals that only Phe-430 is conserved in all CP47 sequences, suggesting that Phe-430 is an important residue for PSII stability in this region.

The situation with Δ(R384-V392) is somewhat different. It has previously been reported that the deletion between Arg-384 and Val-392 leads to an impaired binding of PSII-O to the photosystem (*40*). However, it is clear from the data shown here that PSII-O is functionally associated with PSII in Δ(R384-V392) and no apparent inhibition of photoautotrophic growth could be detected in calcium-limiting BG-11 which prevented the growth of strains in which the PSII-O protein was absent. Following the removal of PSII-O in Δ-(R384-V392), the rate of oxygen evolution at 700 $\mu E \cdot m^{-2} \cdot s^{-1}$ was observed to decrease although the number of assembled PSII centers detected by herbicide-binding experiments remained essentially unchanged. Therefore, although PSII activity appears to be further inhibited by the removal of PSII-O in Δ(R384-V392), the stability or assembly of the photosystem appears to be unaffected.

Arginine-384 is present in all CP47 sequences currently in the database, and Arg-385 is highly conserved with the only difference being the substitution of a Lys at position 385 in *Chlamydomonas*. Mutation of this positive charge pair produces a specific lesion on the donor side of PSII without significantly destabilizing the PSII complex in *Synechocycstis* sp. PCC 6803, and it has been suggested that the phenotype of Δ(R384-V392), with respect to oxygen evolution activity, can be accounted for by alterations at Arg-384 and Arg-385 (*41*, *42*). Recently, Qian et al. (*43*) have shown that the quantum yield of photoactivation in the double Arg to Glu mutant, RR384385EE, increased in a fashion similar to that reported for their *psb*O deletion mutant (*44*) and that these two mutations affected a similar process in a manner that was not additive when the two mutations were combined. This observation has been ascribed to RR384385-EE reducing the binding of PSII-O to the thylakoid and thereby facilitating the access of Mn to the active site for the assembly of the tetranuclear Mn cluster as suggested for the *psb*O deletion mutant (*43*). However, the opposite result was obtained with Δ(R384-V392) when photoactivation was measured (*45*). In Δ(R384-V392), the quantum yield of photoactivation was considerably reduced when compared to the wild type. This result suggests that other amino acids between Arg-384 and Val-389, or amino acids perturbed as a result of the deletion in Δ(R384-V392), are important for the photoactivation process (*45*). The existence of phenotypic differences between RR384385EE (or RR384385GG) and Δ(R384-V392) suggests that further studies focused on the other amino acids in this region are warranted. In Figure 8, it can be seen that the residues between Arg-384 and Val-389 are quite highly conserved, notably Glu-387 and Ser-391, but Lys-389 has also been implicated as an important amino acid through proteolytic digestion experiments and cross-linking studies (*5*, *46*).

Cytochrome *c*-550, or PSII-V, has been shown to be important for the stability of PSII (*5*, *11*, *47*), and our results point to a role for PSII-V in moderating the susceptibility of PSII to photoinactivation. In addition, the removal of PSII-V from either Δ(R384-V392) or Δ(G429-T436) produced an obligate photoheterotrophic phenotype. However, in the case of Δ(R384-V392):ΔPSII-V, a significant number of PSII centers assembled, but despite the ability of these centers to evolve a small amount of oxygen when illuminated at 700 $\mu E \cdot m^{-2} \cdot s^{-1}$, they were unable to support photoautotrophic growth.

The Role of Individual Amino Acids between Gly-351 and Thr-365. Deletion of Gly-351 to Thr-365 produced the obligate photoheterotrophic strain Δ(G351-T365) (*19*). Given the fact that this domain overlaps with the domain known to be recognized by the monoclonal antibody FAC2, as shown in Figure 1, it seemed plausible that amino acids between Gly-351 and Thr-365 could play an important role in PSII function. Recently the conserved charged residues in this region were mutated, but no significant phenotypic effect was detected (*42*, *48*). In addition, the replacement of Pro-360 by Gly did not alter photoautotrophic growth. This led to the suggestion that the reason for the phenotype of Δ(G351-T365) was simply that a large number of amino acids had been removed, thus introducing a detrimental positional effect (*48*). In Figure 3, however, we were able to demonstrate that when we complemented the mutation that created the strain Δ(G351-T365) with a pair of oligonucleotides, carrying defined amino acid substitutions, photoautotrophic growth was restored when the oligonucleotides inserted in the correct orientation but not when they inserted in the reversed direction. This suggests that the positional interpretation for the phenotype of Δ(G351-T365) is insufficient to explain all the experimental evidence. The quasi-random amino acid sequence introduced between Gly-351 and Thr-365 in the strain QRM-2 could not substitute for the wild-type sequence.

In Figure 8, the *Synechocystis* sp. PCC 6803 sequence is shown to be unique in possessing three Glu residues between Gly-351 and Thr-365, and the effect of changing these residues to Gln was investigated by introducing three sets of complementary oligonucleotides that created the strains G351L/E353Q/E355Q/T365Q, G351L/E364Q/T365Q, and the control strain G351L/T365Q. Although Gly-351 is conserved in all CP47 sequences, and Thr-365 is also a highly conserved residue, G351L/T365Q was found to have a similar phenotype to that of the control strain both in the presence and in the absence of PSII-O and PSII-V. Likewise, the evidence collected suggests that both Glu-353 and Glu-355 are not of major functional or structural significance. In contrast, the importance of Glu-364 in CP47 is illustrated by a comparison of the data obtained for G351L/E353Q/E355Q/T365Q and G351L/E364Q/T365Q in the absence of either of the extrinsic proteins. To confirm the importance of Glu-364, the strains E364Q:ΔPSII-V and E364G:ΔPSII-V were also constructed. As with Δ(R384-V392):ΔPSII-V and G351L/E364Q/T365Q:ΔPSII-V, these strains were able to support oxygen evolution at 700 $\mu E \cdot m^{-2} \cdot s^{-1}$ but were unable to support photoautotrophic growth. Several other mutants that have been shown to be associated with the donor side of PSII also retain oxygen-evolving activity even though they fail to grow photoautotrophically (*30*, *49*), but an explanation for these observations has yet to be ascertained. It also remains to be established if the phenotype observed here is unique for substitutions at Glu-364 or whether other amino acid substitutions within the FAC2 epitope produce a similar result.

The Relative Importance of PSII-V. The phenotypes of Δ(R384-V392):ΔPSII-V and G351L/E364Q/T365Q:ΔPSII-V are more severe than the corresponding strains lacking PSII-O. While this result points to the possible existence of significant protein−protein interactions between the domain Glu-364 and Val-392 and cytochrome *c*-550, cross-linking studies with 1-ethyl-3-[3-(dimethylamino)propyl]carbodiimide did not detect any cross-linked products between CP47 and PSII-V (*50*). Therefore, the deleterious effects observed, though clearly significant, may be relayed indirectly from another site of interaction between PSII-V and the PSII complex. An equally possible explanation is that the observed effect arises from a specific role for the PSII-V protein in protecting PSII in vivo. As a result, the removal of PSII-V exacerbates the consequences of the mutations in Δ(R384-V392) and the strains carrying substitutions at Glu-364. With this in mind, it is interesting to consider that cytochrome *c*-550 was not reported to be present in an oxygen-evolving core preparation from *Synechocystis* sp. PCC 6803, suggesting that it is not required for function in vitro (*51*); however, the recent deletion of *psb*V in a PSI-minus strain of *Synechocystis* sp. PCC 6803 resulted in a 7-fold inhibition of PSII activity and a 3-fold reduction in the apparent number of PSII centers (*52*). In addition, PSII-V (and PSII-O) may be required for PSII-U to bind to PSII, and therefore the absence of PSII-U may also be contributing to the phenotypes reported here (*12*, *53*).

Summary. The present study has shown that deletions in loop E of CP47 that produce photoautotrophic mutants can respond differently to the removal of the PSII-O or PSII-V proteins. In the absence of PSII-O, the mutant Δ(G439-T436) failed to assemble PSII reaction centers that could be detected either by herbicide-binding assays or by measurements of variable chlorophyll fluorescence yield. In contrast, the strain Δ(R384-V392), which introduced a lesion in PSII electron transport, did not exhibit a significant difference in its ability either to support photoautotrophic growth or to assemble PSII reaction centers when PSII-O was removed. However, both Δ(R384-V392) and Δ(G429-T436) were unable to grow photoautotrophically in the absence of PSII-V. While this correlated with an absence of assembled PSII in Δ(G429-T436):ΔPSII-V, the strain Δ(R384-V392):ΔPSII-V assembled PSII centers that could not support photosynthesis in vivo. The omission of chloride from the BG-11 medium prevented photoautotrophic growth in Δ(G429-T436) and significantly impaired photoautotrophic growth in Δ(R384-V392). In contrast, calcium-limiting medium appeared to have no detrimental effect on these strains. However, no strains lacking either PSII-O or PSII-V could grow under chloride-limiting or calcium-limiting conditions. Mutation of the conserved residue Gly-351 and the residues Glu-353, Glu-355, and Thr-365 did not produce an altered phenotype in *Synechocystis* sp. PCC 6803 under the conditions evaluated in this study. However, substitution of the conserved Glu-364 by Gln in the strain G351L/E364Q/T365Q severely impaired the stability and/or assembly of PSII in the absence of PSII-O and entirely prevented

photoautotrophic growth in the absence of PSII-V, although a limited ability to evolve oxygen was retained. The construction of the two mutants E364Q:ΔPSII-V and E364G:ΔPSII-V established that this inhibition was a consequence of the mutation at Glu-364.

ACKNOWLEDGMENT

We thank Prof. Wim Vermaas for the gift of the *psb*V deletion construct and Prof. Bridgette Barry for the gift of the PSII-O antibody.

REFERENCES

1. Bricker, T. M., and Ghanotakis, D. F. (1996) in *Oxygenic Photosynthesis*: *The Light Reactions* (Ort, D. R., and Yocum, C. F., Eds.) pp 113−136, Kluwer Academic Publishers, Dordrecht.
2. Hankamer, B., Barber, J., and Boekema, E. J. (1997) *Annu. Rev. Plant Physiol. Plant Mol. Biol. 48*, 641−671.
3. Britt, D. R. (1996) in *Oxygenic Photosynthesis*: *The Light Reactions* (Ort, D. R., and Yocum, C. F., Eds.) pp 137−164, Kluwer Academic Publishers, Dordrecht.
4. Ikeuchi, M., Shukla, V. K., Pakrasi, H. B., and Inoue, Y. (1995) *Mol. Gen. Genet. 249*, 622−628.
5. Seidler, A. (1996) *Biochim. Biophys. Acta 1277*, 35−60.
6. Ono, T., and Inoue, Y. (1984) *FEBS Lett. 162*, 281−286.
7. Miyao, M., and Murata, N. (1984) *FEBS Lett. 170*, 350−354.
8. Kuwabara, T., Miyao, M., Murata, T., and Murata, N. (1985) *Biochim. Biophys. Acta 806*, 283−289.
9. Ghanotakis, D. F., Babcock, G. T., and Yocum, C. F. (1984) *FEBS Lett. 167*, 127−130.
10. Miyao, M., and Murata, N. (1985) *FEBS Lett. 180*, 303−308.
11. Shen, J.-R., Vermaas, W. F. J., and Inoue, Y. (1995) *J. Biol. Chem. 270*, 6901−6907.
12. Shen, J.-R., Ikeuchi, M., and Inoue, Y. (1997) *J. Biol. Chem. 272*, 17821−17826.
13. Bricker, T. M. (1990) *Photosynth. Res. 24*, 1−13.
14. Odom, W. R., and Bricker, T. M. (1992) *Biochemistry 31*, 5616−5620.
15. Bricker, T. M., and Frankel, L. K. (1987) *Arch. Biochem. Biophys. 256*, 295−301.
16. Frankel, L. K., and Bricker, T. M. (1989) *FEBS Lett. 257*, 279−282.
17. Frankel, L. K., and Bricker, T. M. (1992) *Biochemistry 31*, 11059−11063.
18. Vermaas, W. F. J., Ikeuchi, M., and Inoue, Y. (1988) *Photosynth. Res. 17*, 97−113.
19. Eaton-Rye, J. J., and Vermaas, W. F. J. (1991) *Plant Mol. Biol. 17*, 1165−1177.
20. Mayfield, S. P., Bennoun, P., and Rochaix, J.-D. (1987) *EMBO J. 6*, 313−318.
21. Burnap, R. L., and Sherman, L. A. (1991) *Biochemistry 30*, 440−446.
22. Philbrick, J. B., Diner, B. A., and Zilinskas, B. A. (1991) *J. Biol. Chem. 266*, 13370−13376.
23. Mayes, S. R., Cook, K. M., Self, S. J., Zhang, Z., and Barber, J. (1991) *Biochim. Biophys. Acta 1060*, 1−12.
24. Bockholt, R., Masepohl, B., and Pistorius, E. K. (1991) *FEBS Lett.* 294, 59−63.
25. Shen, J.-R., Burnap, R. L., and Inoue, Y. (1995) *Biochemistry 34*, 12661−12668.
26. Rippka, R., Deruelles, J., Waterbury, J. B., Herdman, M., and Stanier, R. Y. (1979) *J. Gen. Microbiol. 111*, 1−61.
27. Williams, J. G. K. (1988) *Methods Enzymol. 167*, 766−778.
28. MacKinney, G. (1941) *J. Biol. Chem. 140*, 315−322.
29. Vermaas, W. F. J., Charité, J., and Shen, G. (1990) *Z. Naturforsch. 45C*, 359−365.
30. Nixon, P. J., and Diner, B. A. (1992) *Biochemistry 31*, 942−948.
31. Nishiyama, Y., Kovács, E., Lee, C. B., Hayashi, H., Watanabe, T., and Murata, N. (1993) *Plant Cell Physiol. 34*, 337−343.
32. Laemmli, U. K. (1970) *Nature 277*, 680−685.
33. Vermaas, W. F. J., Charité, J., and Eggers, B. (1990) in *Current Research in Photosysnthesis* (Baltscheffsky, M., Ed.) Vol. 1, pp 231−238, Kluwer Academic Publishers, Dordrecht.
34. Prentki, P., and Krisch, H. M. (1984) *Gene 29*, 303−313.
35. Elhai, J., and Wolk, P. (1988) *Gene 68*, 119−138.
36. Engels, D. H., Lott, A., Schmid, G. H., and Pistorius, E. K. (1994) *Photosynth. Res. 42*, 227−244.
37. Larson, G. F., Fassel, V. A., Scott, R. H., and Knisely, R. N. (1975) *Anal. Chem. 47*, 238−243.
38. Celon, E., and Bresadola, S. (1969) *Mikrochim. Acta 1969*, 441−448.
39. Haag, E., Eaton-Rye, J. J., Renger, G., and Vermaas, W. F. J. (1993) *Biochemistry 32*, 4444−4454.
40. Gleiter, H. M., Haag, E., Shen, J.-R., Eaton-Rye, J. J., Inoue, Y., Vermaas, W. F. J., and Renger, G. (1994) *Biochemistry 33*, 12063−12071.
41. Putnam-Evans, C., and Bricker, T. M. (1992) *Biochemistry 31*, 11482−11488.
42. Putnam-Evans, C., Burnap, R., Wu, J., Whitmarsh, J., and Bricker, T. M. (1996) *Biochemistry 35*, 4046−4053.
43. Qian, M., Al-Khaldi, S. F., Putnam-Evans, C., Bricker, T. M., and Burnap, R. B. (1997) *Biochemistry 36*, 15244−15252.
44. Burnap, R. L., Qian, M., and Pierce, C. (1996) *Biochemistry 35*, 874−882.
45. Gleiter, H. M., Haag, E., Shen, J.-R., Eaton-Rye, J. J., Seeliger, A. G., Inoue, Y., Vermaas, W. F. J., and Renger, G. (1995) *Biochemistry 34*, 6847−6856.
46. Hayashi, H., Fujimura, Y., Mohanty, P., and Murata, N. (1993) *Photosynth. Res. 36*, 35−42.
47. Nishiyama, Y., Hayashi, H., Watanabe, T., and Murata, N. (1994) *Plant Physiol. 105*, 1313−1319.
48. Putnam-Evans, C., Wu, J., and Bricker, T. M. (1996) *Plant Mol. Biol. 32*, 1191−1195.
49. Putnam-Evans, C., and Bricker, T. M. (1997) *Plant Mol. Biol. 34*, 455−463.
50. Han, K.-C., Shen, J.-R., Ikeuchi, M., and Inoue, Y. (1994) *FEBS Lett. 355*, 121−124.
51. Tang, X. S., and Diner, B. A. (1994) *Biochemistry 33*, 4594−4603.
52. Manna, P., and Vermaas, W. (1997) *Plant Mol. Biol. 35*, 407−416.
53. Shen, J.-R., and Inoue, Y. (1993) *Biochemistry 32*, 1825−1832.
54. Devereux, J., Haberli, P., and Smithies, O. (1984) *Nucleic Acids Res. 12*, 385−398.
55. Jameson, B., and Wolf, H. (1988) *Comput. Appl. Biosci. 4*, 181−186.

BI980404S